

The Effect of Shape Variables of Tibial Plateau on Tibio-femoral Movement Based on a Three-dimensional Anatomical Dynamic Model

N. Ekin Akalan^{1,2}, Mehmed Özkan³, Yener Temelli²

¹Gait analysis Laboratory Physical Therapy Center, Dept. of Developmental Child Neurology, School of Medicine Istanbul University, İstanbul, Turkey

²Dept. of Orthopedics and Traumatology School of Medicine Istanbul University, İstanbul, Turkey

³Institute of Biomedical Engineering, Boğaziçi University, İstanbul, Turkey

Abstract. In this study the geometric and material properties of joint surfaces, bones, ligaments of the tibio-femoral joint is represented and passive knee flexion is simulated. The purpose of the study is to observe the effect of 11° tibial slope to the tibio-femoral movement. The contact forces between tibia and femur are defined as frictionless mathematical model. Tibial plateaus and condyles of femur are represented as ellipsoids as described in literature. Anterior, posterior cruciate ligaments, medial, lateral collateral ligaments are represented as non linear elastic springs. Knee flexion with and without internal-external torque are simulated, and the results are compared with the literature for sloped and flattened medial tibial plateau models. As a result, normal internal rotation of tibia and adduction ranges are achieved for unloaded condition in flattened model, but the knee flexion with forced internal/external rotation are out of normal range for both models.

1 Introduction

It is well known that the mathematical models play an important role for the understanding of complicated biological structures. The human knee has a complex anatomical structure and complicated three dimensional movements. Not only a faithful description of normal function, but also identification of and treatment of dysfunction presents many problems [21]. It has proved challenging to measure and then to depict knee joint motion [7]. The four bar theory based kinematical models developed by [22], [12] and [8]. In this type of model force action in the structures of the joint is not considered.

[6] studied on force action between structures, but kinematic behavior of the knee is considerably simplified. Morrison represented the knee as a simple hinge joint [1]. In the model of [6], the motions in the joint were based on experimental data in the literature. However the contribution of the curved joint surfaces to the mechanical behavior was ignored in all these models [7, 12, 22].

[2] developed a model to analyze the movement and the force changes of the knee by employing finite element method. The ligaments, joint capsules were modeled as nonlinear springs while the joint surfaces were modeled by a number of flat surfaces. The studies of the kinematic knee modeling continued until wide spread use of MRI scanning [7, 18].

MRI screening provided a huge improvement on analyzing 3D knee kinematics. [7] defined the natural knee movements based on MR images of the knee. This study illustrates, defining the natural movement of the knee plays a very important role for understanding the effectiveness of prosthesis, rehabilitation and surgery on joint pathologies. Unfortunately simulation of passive knee movement by representing natural anatomic structures and their 3D geometries has not been published, yet. Even though tibial plateau was represented by flat [1, 6, 16] and uneven [5, 6, 11] surfaces by different studies, there are no studies comparing the superiority of either of the uneven or flat surfaces. There has already been extensive work on the kinematics of tibio-femoral joint, however the most detailed geometric shape representation of the femoral and tibial surface which was previously studied by Freeman and Pinskerova was not modeled to analyze tibio-femoral flexion.

The objective of our study is to create a dynamic 3D knee model which represents tibio-femoral joint surfaces, bones and ligaments by the consideration of their geometric and material properties to simulate 0°-90° passive knee flexion.

2 Materials and Methods

The model created has the characteristic as; 1.80 cm tall, 80 kilograms, 18 years old human's volume rendered shell files, the locations of their center of mass, inertial moments of the right femur and right tibia are provided from BRG*. All the files are imported into MSC. ADAMS software [19]. The foot segment was also imported to the ADAMS software except the shell file to decrease the load to the computer during simulation.

2.1 Geometric and Contact Conditions

Femoral condyles represented as spheres as defined Freeman and [15]. In this study, medial femoral condyle is represented as two ellipsoids; 22mm for flexor facet radii, 32mm for extensor facet radii. Lateral femoral condyle ellipsoid is represented as two spheres 21mm for flexor facet radii, 32mm for extensor facet radii. According to the work medial femoral condyle divided in to 3 sections; Extensor Facets 49°, Flexor facets 110° and Posterior horn facets 24°. The lateral femoral condyle has 3 sections; Extensor Facets [EF] 32°, Flexor facets [FF] 114° and Posterior Horn Facets [PHF] 33°. Medial tibial plateau has 4 sections; Anterior Horn Facets [AHF] 9mm, Extensor facet [EF] 17mm, Flexor Facets [FF] 10mm, Posterior Horn Facet [PHF]15mm. Extensor facet slopes upwards and forwards by 11° relative to posterior, roughly

* LifeMOD Biomechanics Modeler database.

horizontal surface. Lateral tibial plateau has 3 sections; Anterior Horn Facet 11mm, Tibial Articular Facet [TAF] 24mm, Posterior Horn Facet 11mm [7, 9] (Figure 1).

In the present work femur is assumed to be fixed and tibia moves relative to the femur and gravity is assumed to be opposite direction in order to contact continued between femur and tibia during flexion. The tibia is assumed to begin its motion from rest while the knee was fully extended.

Friction forces are neglected because of the extremely low coefficient of friction of articular surfaces [1].

In the absence of joint axial compressive loads the effect of menisectomy on joint motion is minimal compared with that of cutting ligaments [16]. Since loading conditions are limited to those where the knee joint is not subjected to external axial compressive loads, the menisci thus not included in the present model [1].

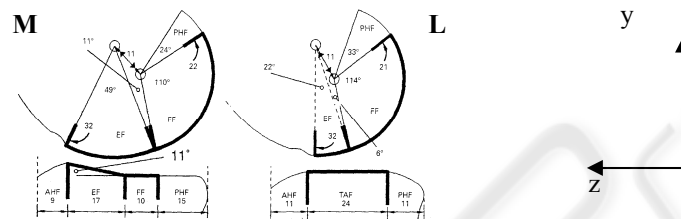


Fig. 1. Diagram of sagittal sections of medial [left] and lateral [right] tibio-femoral components.

The contact force between tibia and femur is formalized as:

$$F_n = k [g^e] + \text{step}[g, 0, 0, d_{\max}, c_{\max}] dg/dt \quad (1)$$

where k [46.58 N/mm] is the stiffness coefficient, g is penetration [mm], e [4] is a force exponent, d_{\max} [1cm] is the penetration limit c_{\max} is the maximum damping coefficient [97.19 N/mm/sec], dg/dt is the penetration velocity.

Patton [1993] took the penetration length as 1 cm for foot, but Blankevoort et al [5] revealed that the articulate thickness for the knee is 2 mm, so 50% of the cartilage thickness as penetration length is taken.

The single component force is applied to flex the knee from the center of mass of the tibia as presented in [1] and Blankevoort et.al. [1, 5-6].

$$F_q = A e^{-4.75[t/t_0]^2} \sin[\pi t/t_0] \quad (2)$$

where A and t_0 are the amplitude and the pulse duration, respectively. Forcing pulses of this can be simulated experimentally. Forcing pulse duration is assumed as 140N and 0.1 respectively.

A co-ordinate system for the normal knee based on posterior femoral circles has been proposed by [11]. The origin is located at the center of the posterior spherical portion of the medial femoral condyle so that the origin of the system approximately coincides with the center of rotation of the knee as defined in [7].

2.2 Ligamentous Forces

The model includes 13 nonlinear spring elements which represent different ligamentous structures and capsular tissue posterior of the knee joint. Four of them stand for the respective anterior and posterior fiber bundles of anterior cruciate ligament [ACL] and the posterior cruciate ligament [PCL]; another four represent the deep, oblique, anterior and posterior fiber bundles of the medial collateral ligament [MCL], one spring represents the lateral collateral ligament [LCL], and four elements represent the medial, lateral, oblique fiber bundles of posterior part of the capsule [CAP]. The local co-ordinates of the femoral and tibial insertion sites of the ligamentous structures are specified according to the data available in the literature [3,5,15].

Ligament assumed to be a line element extending from the femoral origin to tibial insertion, wrapping around the bone surfaces is not taken into account.

In the present study the ligaments are determined according to the force length relationship as [21]

$$F_j = \begin{cases} 0; & \epsilon_j \leq 0 \\ K1_j(L_j - L_{0j})^2; & 0 = \epsilon_j \leq 2\epsilon_1 \\ K2_j[L_j - (1 + \epsilon_1)L_{0j}]; & \epsilon \geq 2\epsilon_1 \end{cases} \quad (3)$$

where ϵ_j is the strain in the j th element, $K1_j$ and $K2_j$ are the stiffness coefficients of the j th spring element for the parabolic and linear regions, respectively, and L_j and L_{0j} are its current and slack lengths, respectively. The linear range threshold is specified as $\epsilon_1 = 0.03$ [1,4,13].

Values of the stiffness coefficients of the spring elements used to model the different ligamentous structures are taken from the data available in the literature [1]. The slack length of each spring element is obtained by assuming an extension ratio ϵ_j at full extension and using it to evaluate the spring element's slack length, L_{0j} , from its length at full extension which can be calculated from the coordinates of the attaching points. The values of the extension ratios are specified according to the data available in the literature [3,5]. It is verified that the selected extension ratios did not produce nonanatomical strains [i.e., strain levels that indicate ligamentous failure] over the whole range of motion.

3 Results

The comparison of internal and external rotation during passive knee flexion data are shown in Figure 2. The behavior of the graphics of flat surfaces simulation and natural rotation of tibia are different. In [7] based simulation, tibial rotation is lower than normal during knee flexion. Tibial internal rotation is around 2 - 4° between 10 - 40° of knee flexion and rotated internally between 40 - 65°. Even though 65° knee flexion tibial rotation is trying to catch the normal rotation, tibia has reached only 12° internal rotation which is below the normal according to [20].

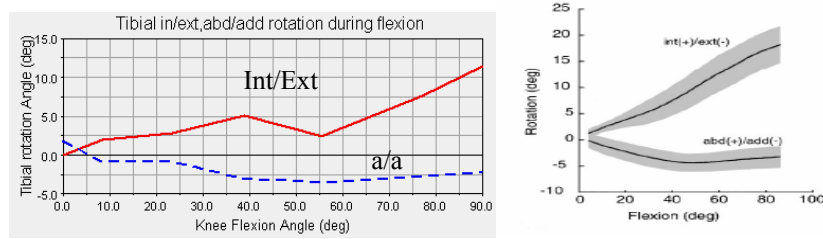


Fig. 2. Comparison of int-ext rotation during knee flexion. Freeman and Pinskrova based simulation (left), and Knee rotation from Wilson et. al.(right).

In simulation based on Freeman and Pinskerova translations, tibial attachment of pACL is in range except the antero-posterior translation in first 20° flexion. Tibia translated forward during the first 20° where it is expected to translate to the backward (Figure 3).

11° slope of tibial external facet is removed and the surface of the external facet and the posterior part of the tibia provided to be on the same level. So that magnitude of tibial internal rotation increased (Figure 4).

The internal rotation and adduction during the knee flexion is in range of normal knee which revealed in Wilson et al 24.

The translation of tibial insertion point of pACL relative to femur during knee flexion is in the range of normal translation described in Wilson et al's work (Figure 5). The backward translation of pACL attachment reduced

Position of medial and lateral condyle contact point is simulated as in Pinskerova 2000. Medial femoral EF to FF rock occurred at 36°, femoral FF is in contact with tibial FF from 36° to 90° knee flexion.

Lateral Femoral EF to FF rock occurred around 5° and from 5 to 90° femoral FF is in contact with the tibia in sloped model. EF to FF rock is occurred at 10° flexion in flattened tibial surface. After 10° FF contact lasts till 90° as in the literature [11]. For the flattened medial tibial surface EF to FF rock occurred at 30° flexion and FF contact with femoral FF till 120° flexion as revealed in Pinskerova et al work 2000

To analyze the behavior of the knee under loading conditions, 3Nm internal and external force applied from the location of tibial center of mass as described in Blankevoort et al [4-7]. The results for the model with and without 11° slope is compared to the literature results (Figure 5) [5].

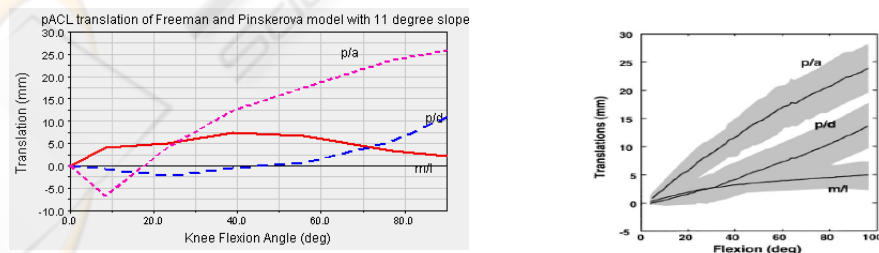


Fig. 3. Comparison of simulation with 11° slope (left) and Knee rotation from Wilson et. al.(right).

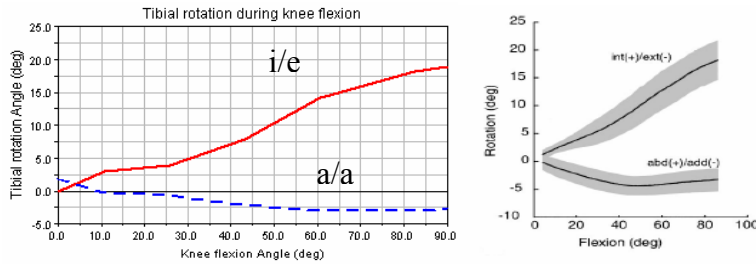


Fig. 4. Natural internal rotation during knee flexion after 11° slope is removed.

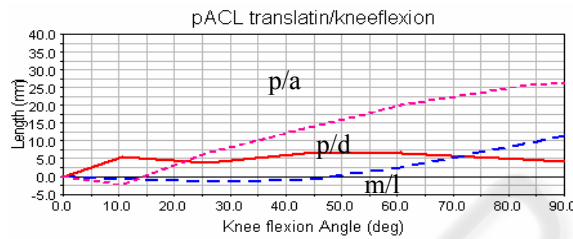


Fig. 5. Translation of pACL during knee flexion. Freeman and Pinskrova based simulation.

Tibial internal rotation is increased linearly and reached 60° tibial rotation at 90° knee flexion, external rotation with 3Nm external torque is in normal range for the Iwaki and Pinskerova based simulation [9].

Even though tibial internal rotation with 3Nm torque is in normal range, tibial external rotation is lower than normal after 35° of flexion for external rotation torque in simulation without 11° tibial slope.

Knee varus / valgus rotation during the application of 3 Nm internal/external rotational torque is also studied. The results are compared with Blankevort et al (Figure 6) [6].

According to the results, valgus occurs with internal load and with external load till 75° knee flexion for 11° tibial slope. After 75° flexion valgus rotation is observed. Valgus rotation is seen for internal and external load after 30° flexion for flattened medial tibial surface model. Before the 30° flexion valgus rotation has occurred (Figure 6).

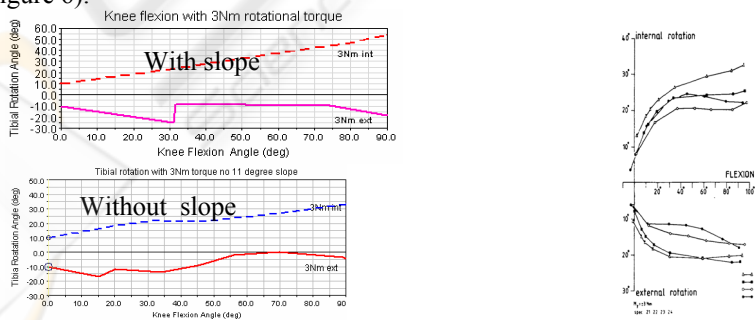


Fig. 6. Comparison of 3Nm loading torque with Blankevoort et al, Freeman and Pinskrova based simulation (left), and Knee rotation from Blankevoort et. al.[1991](right).

4 Discussion

A review of the literature reveals that there is no published anatomical dynamic knee model based on Freeman et al works [4] which describes the anatomy of the articular surfaces and their movement in the normal tibio-femoral joint by some combination of MRI, CT, RSA or fluoroscopy. During building anatomical dynamic knee model, natural tibial rotation is achieved by removing 11° tibial slope. The aim of the study is to observe the effect of 11° tibial slope to the tibio-femoral movement and to build the most carefully sectioned tibio-femoral dynamic knee model by guidance of Freeman et al 2005.

Tibial internal rotation during knee flexion is lower than the normal with 11° slope. The slope on the medial tibial surface decreases the rotation by blocking tibial internal rotation and allowing external rotation in $0 - 40^\circ$ knee flexion. Between $40 - 65^\circ$, 11° slope tackles the medial flexor facet and pushes the tibia into its external rotation. After 65° contact moves to the posterior tibial surface and faster internal rotation is occurred.

For the flat surface tibia demonstrated natural internal rotation. Abduction and adduction rotation with and without 11° medial tibial slope are in the allowed limits (Figure 2, 4).

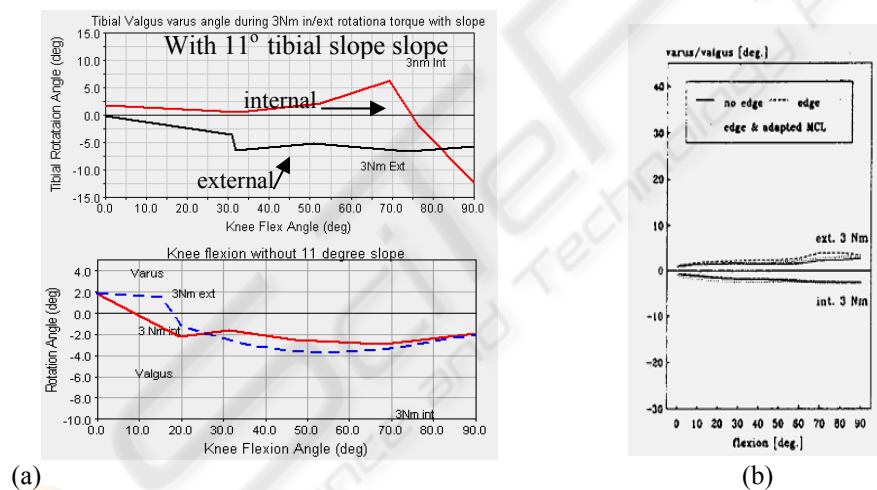


Fig. 7. Comparison of internal and external 3Nm loading torque on a) valgus / varus rotation with and without 11° tibial slope, b) Blankevoort et. al. (right).

Translation of most posterior location of anterior cruciate ligament is followed. Antero-posterior translation is in normal range except first 20° part of knee flexion in original model. In 20° knee flexion, tibia moves forward instead of backward in the sloped model. The backward movement might be resource from hitting EF to the slope and produce a contra force to forward motion. It may be a cause of damping coefficient of contact formulation, which make tibia jump on femoral EF. Due to the absence of the slope, smoother forward movement occurs in flat tibial surface.

Position of each part of the lateral and medial plateau relative to femur during knee flexion is specially revealed in Pinskerova et al 2000. For the medial components; from 0 - 10°: Femoral EF contacts with tibial EF, from 10 - 30°: EF should be rock to FF, from 30 - 120°: Femoral FF is in contact with tibial FF. EF to FF femoral rock occurring at 36° in simulation with slope which was late relative to the normal. EF to FF rock at 30° knee flexion in flattened tibial model. After that, the rock contact match with literature [9,15].

For the lateral compartment; from 0 - 10° EF, or FF in absence of EF, should be in contact [5]. Femoral FF-to-FF rock is occurred at 5°, 10° flexion in slopped and is flattened model respectively which are within the allowed limits. From 10 to 90° FF is in contact with the tibia, over 90° tibia contact shared with PHF [17]. After the 10° FF is in contact with tibial FF as literature.

To analyze loading conditions on both models, 3Nm rotational torque was applied [5]. Higher and a linear manner tibial internal rotation is seen with internal load and lower external rotation for external load in slopped model. Tibial internal rotation is in range during internal load in flattened tibial model. However the external rotation was decreased in flattened model.

The coefficients of the ligaments are obtained directly from the Abdel-Rahman and Hefzy 1998, but the co-ordinates of the ligament attachments taken from Crowninshield et al 1976. In Crowninshield et al 1976 medial collateral ligament is represented as four fibers which are anterior, posterior, deep and oblique although Abdel-Rahman and Hefzy 1998 MCL represented as three fibers, posterior fiber is missing. In our study anterior fiber coefficients is used for posterior and anterior fibers to compensate the absence of posterior fiber. Arcuate popliteal ligament of posterior capsule which represented in Abdel-Rahman and Hefzy 1998 is not included because of absence of location co-ordinates in Crowninshield et al 1976. The reason of obtaining coordinates of ligament attachments from Crowninshield et al 1976 is the origin co-ordinates are not defined clearly in Abdel-Rahman and Hefzy 1998.

Valgus rotation occurs by applying external rotational torque, varus by internal rotational torque [5]. Valgus rotation and first 75° varus rotation by ± 3 Nm rotational torque are in normal range for slopped model. The reason of varus rotation after 75° is the sliding of medial tibial plateau backward and the loss of contact with flexor facet.

Valgus rotation is seen with internal rotation torque as normal although varus rotation is only seen in 30° flexion in flattened tibial model. Valgus rotation is observed by external rotation load after 30°. The reason of varus rotation might be resource from excessive ligament strain or anatomical inefficiencies.

Coronal and transverse plane representation is not clear as sagittal plane in Freeman, Pinskerova and Iwaki [7, 9, 15]. The radii of the spheres for representing tibio-femoral articular surface are also used for coronal plane radii. The radius differences might perform the unnatural valgus rotation by application of external load.

The limitation of the present study is neglecting friction force because of the extremely low coefficient of friction of the articular surface [1]. The MCL is modeled as a straight line segment connecting the femoral and tibial attachments, while the natural MCL wraps around the tibial plateau [20]. Meniscus and joint capsules are not modeled because of their complex structures [2]. Some loads (around 4kg which is weight of shank and foot) are still applied to the knee as it was flexed due to provide

continued contact between tibia and femur by assuming the gravity as upward direction.

The results show that tibial internal rotation during flexion is within the normal limits for the model without 11° anterior tibial slope. Posterior translation of tibial attachment of pACL and sliding and rolling motion of the tibia over femur is near normal range in flattened tibial plateau model. Both models have showed different behaviors in loading conditions. Flattened tibial plateau model is simulated the knee motion within the normal range for unloaded condition.

The primary feature of the three-dimensional dynamic anatomical modeling of the knee is variation of ligament strain to achieve reasonable loading behavior for the knee as revealed in Blankevoort et al. (1991). Modeling of the meniscus, friction, defined in detail contact should be well studied.

Acknowledgements

This project is supported in part by TUBITAK (The Scientific and Technological Research Council of Turkey) grant number 104S508. The project has been coordinated at the Institute of Biomedical Engineering in Boğaziçi University. Gait analysis experiments have been conducted at the Motion Analysis Laboratory of Istanbul University, School of Medicine.

References

1. Abdel-Rahman E.M., Hefzy M.S.: Three-dimensional dynamic behavior of the human knee joint under impact loading J. Biomech 1998, Vol 20, pp.276-90
2. Andriacchi, T.P., Mikosz R.P., Hampton S.J. and Galante O. A statically indeterminate model of the human knee joint, Biomechanics symposium AMD.1977.23,227-239
3. Beynon B, Yu J, Huston D, Fleming B, Johnson R, Haugh L, Pope MH.: A sagittal plane model of the knee and cruciate ligaments with application of a sensitivity analysis. J. Biomech. Eng. 1996; 118:227–39.
4. Blankevoort, L., Huijskes, R., de Lange, A., 1988. The envelope of passive knee joint motion. Journal of Biomechanics 21, 705–720.
5. Blankevoort L., Kuiper J.H., Huijskes R., Grootenboer H.J. Articular contact in a three-dimensional model of knee. J. Biomech 1991, Vol 24, pp.1019-31
6. Crowninshield R. Pope H., Johnson R.J. An analytical model of the knee. . J. Biomech 1976, Vol 9, pp.397-405
7. Freeman M.A.R., Pinskerova V.: The movement of the normal tibio-femoral joint. J.Biomech 2005; 38[2]:197-208.
8. Huson A. Biomechanische probleme des kniegelenks, Orthopade1974;3:119-126
9. Iwaki H, Pinskerova V., Freeman M. Tibia-femoral movement 1: the shapes and relative movements of the femur and tibia in the unloaded cadaver knee. J Bone Joint Surg Br 2000; 82:1189-95
10. Kapandji IA.1970 The physiology of Joints, Churchill Livingstone.2.nd ed.,pp:72-134
11. McPherson,A.,Karrholm,J.,Pinskerova,V.,Sosna,A.,Martelli,S., 2004. Imaging knee motion using MRI, RSA/CT and 3Ddigitization. Journal of Biomech 37, this issue, doi:10.1016/j.biomech.2004.02.007
12. Menschik A. Mechanic des Kniegelenks. 1 Teil,Z. Orthop 1974;112:481-495

13. Moglo, K.E., Shirazi-Adl, A., 2003. Cruciate coupling and screw home mechanism in passive knee joint during extension-flexion *J. Biomech* 2005, May;38(5):1075-83
14. Patton J.L. Forward dynamic modeling of human locomotion .Master thesis 1993 pp:32
15. Pinskerova V, Iwaki H, Freeman M: The shapes and relative movements of the femur and tibia in loaded cadaveric knee: A study using MRI as an anatomical tool. In: *surgery of the knee* Insall JN, Scott WN, eds. 3rd ed. Philadelphia: W.B Saunders Co. 2000
16. Seedhom B.B., Suda Y. Axis of tibial rotation and its change with flexion angle. *Clin Orth* 2000;341:178-182
17. Shelburne K.B., Pandy M.C. A musculoskeletal model of the knee for evaluating ligament forces during isometric contractions. *J Biomech* 1997;30:163-76
18. Smith P.N., Refshauge K.M., Scarvell J.M. Development of concepts of knee kinematics *Arch Phys Med Rehabil* 2003;84:1895-1902
19. The genesis of the LifeMOD® Biomechanics Modeler Virtual Biomechanics Brochure, www.adams.com
20. Wilson D.R., Feikes J.D., Zavatsky A.B., O'Connor J.J. The components of passive movement are coupled to flexion angle *J. Biomech* 2000, Vol 33, pp.465-73
21. Wismans J, Veldpaus and Jansen J: A three dimensional mathematical model of the knee joint. *J Biomech* 1980;13:677-85
22. Zuppingen, H. Die aktive Flexion in unbelasteten Kniegelenk, Wiesbaden-verlag von J.F. Bergmann, 1904

